SPINEL-RICH LITHOLOGIES ON THE MOON: AN EXPERIMENTAL STUDY OF POSSIBLE PRECURSOR MELT COMPOSITIONS J. Gorman[1,2], J. Gross[3,4]; [1]University of Rochester, Rochester NY 14627; [2]now at University of Maryland, College Park, MD 20742; [3]Lunar and Planetary Institute, Houston TX 77058; [4] now at the American Museum of Natural History, New York NY 10024.

Introduction: The lunar crust contains some of the most important and accessible clues to the history of the Moon's chemical evolution [1-3]. The M^3 near-infrared (NIR) imaging spectrometer on the Chandrayaan-1 spacecraft discerned several areas on the rim of the far-side Moscoviense basin which had near-IR reflectance spectra characteristic of abundant $(Mg,Fe)Al_2O_4$ spinel with less than 5% mafic silicate minerals. Pieters et. al. [4] suggested that these deposits represent a previously unknown lunar rock type, spinel anorthosite. However, the origin and mechanism(s) of formation of such spinel-rich rocks are not clear yet.

Recently, a spinel-rich clast in meteorite Allan Hills (ALH) A81005 has been reported; it contains ~30 vol% spinel, the most reported spinel in any lunar sample [5]. Thus, it represents a great opportunity to study the formation of spinel-rich lunar lithologies. Gross and Treiman [10] suggested that this clast formed as a spinel cumulate from a picritic magma body that assimilated crustal anorthosite on its margins. This explains the petrographic and chemical features of the clast [10], and is consistent with the regional setting of the Moscoviense spinel deposit. However, it remains possible that this clast could have formed as a spinel cumulate from an impact melt of troctolitic composition.

Here we present data of liquidus/crystallization experiments at low pressure to provide constraints on the origin and formation history of Mg-Al spinel-rich and spinel-bearing lunar highland samples. Experiments on the bulk composition of ALHA81005 (Table 1) will help us determine if melting of the meteorite source region can produce such spinel-rich rocks. Experiments on the bulk clast composition will reveal whether spinel-rich samples can be melt compositions themselves or if other concentration processes must have taken place in order to enrich the rock in spinel.

Table 1: Representative chemical analyses of experimental run products, ALHA81005 bulk composition.

	1500°C	1400°C	1300°C		1200°C			starting composition
Wt%	glass	glass	glass	plag	glass	plag	olivine	ALHA81005 Bulk
SiO_2	45.30	44.88	45.99	43.86	49.20	42.96	39.16	44.70
TiO_2	0.26	0.26	0.40	0.02	0.86	0.04	0.02	0.25
Al_2O_3	25.00	26.08	19.28	35.53	14.16	35.13	0.91	26.00
FeO	5.11	3.01	7.73	0.26	11.06	0.64	15.41	5.50
MnO	0.08	0.05	0.11	0.01	0.17	0.01	0.18	0.08
MgO	8.08	8.52	12.18	0.45	9.92	0.68	43.50	7.90
CaO	16.11	17.19	14.30	19.83	14.61	20.53	0.82	15.00
Na_2O	0.05	0.01	0.02	0.03	0.01	0.01	0.00	0.20
Total	99.99	100.00	100.01	99.99	99.99	100.00	100.00	99.63

Methods:

Experiments: 1-bar liquidus/crystallization experiments were conducted in a Deltech gas mixing furnace (ARES Laboratory, JSC). The oxygen fugacity was regulated by mixing CO-CO_2 gas to a desired Moon-like fO_2, at ~1 log unit below the iron-wüstite buffer. Synthetic powder starting materials with the bulk compositions of ALHA81005 and the clast 2 composition were made from homogenized mixtures of element oxides. The experiments were held above the liquidus at 1500ºC for several hours up to 1 day and then quenched at 1500ºC, 1400ºC, 1300ºC, 1200ºC, and 1150ºC. The synthetic powder of the ALHA81005 bulk composition was fired and completely melted at 1-bar and quenched to a homogeneous anhydrous glass before the experimental run. The glass was grounded to powder and remixed to ensure homogeneity.

The synthetic powder of clast 2 bulk composition could not be melted to a glass before the experimental run due to technical problems with the furnace. Thus experiments on this composition were conducted directly from the oxide mixtures.

Phase abundances: To determine mineral abundances and ensure that no phases are missed during EMPA analysis, we performed mass balance calculations using the least squares method. Equilibrium-distribution-coefficients were calculated for olivine-glass (liquid), $K_{DFeO\text{-}MgO} = [X_{FeO(Ol)}X_{MgO(L)}] / [X_{MgO(Ol)}X_{FeO(L)}]$.

EMP: Cameca SX100 electron microprobe analysis was used to obtain backscattered electron images and quantitative chemical analyses. Quantitative analyses were obtained by wavelength dispersive spectrometry. Operating conditions were 15kV accelerating voltage, and 20nA beam current.

Experimental Results:

ALHA81005: The results of the 1-bar experiments on ALHA81005 bulk composition show that spinel does not crystallize from the starting material. The bulk composition plots in the plagioclase field (Fig. 1). Thus, plagioclase should be the first phase to crystallize; olivine the second phase, and (presumably) pyroxene would follow at temperatures lower than in our experiments. The Experimental run products confirm this as (Fig. 2) the run products include glass, plagioclase and olivine in different proportions, with 100vol% glass at 1500ºC decreasing to 33vol% glass at 1200ºC while plagioclase and olivine increase to 57vol% plagioclase and 10vol% olivine at 1200ºC (Fig. 2).

Clast 2: The results of the 1-bar experiments on clast 2 show spinel crystallization at all experimental temperatures. The bulk composition plots outside the SiO_2-Olivine-Plagioclase diagram due to the enrichment in spinel. Spinel is the first phase to crystallize; its abundance reaches a maximum of 30vol% at 1500ºC. Olivine is the second phase to crystallize, followed by plagioclase at 1200ºC. However, backscattered images (BSE) of the experimental product show swirls and pockets of different melt compositions. Calculated distribution-coefficients for olivine-glass show a wide range of K_D = 0.27 up to 0.90.

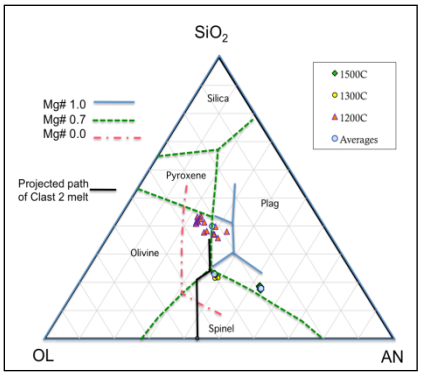

Figure 1: Phase diagrams for the olivine-anorthite-silica, projection after Longhi (1977, Fig. 2a). Liquidus boundaries shown for several values of Mg#. Data points are glass compositions for experiments on the ALHA81005 bulk composition. Black solid line represents the melt composition path of clast 2 melt.

Discussion and Implications: The observation of new lunar lithologies on the lunar surface is one of the more intriguing discoveries raising new questions about igneous processes in the lunar crust. Especially perplexing is the question of how spinel-rich samples such as the spinel-rich fragment in ALHA81005 [5, 10] and the spinel-rich deposits detected by M^3 [4] fit into the petrogenetic schemes? Do they represent material that was excavated by an impact from deep within the crust or do they represent crystallized material from an impact melt sheet?

ALHA81005: The calculated distribution-coefficients for olivine-glass (liquid) fall within the expected range for equilibrium (0.3-0.35), thus it is safe to assume that they were in equilibrium with the melt [12,13]. However, the experiments show that melting and crystallization of the meteorite composition, and hence its presumed source region (e.g. as in an impact melt sheet), will not produce any spinel and thus will not lead to spinel-bearing or spinel-rich lithologies.

Clast 2: Using the oxide mix as a starting material rather than a homogenized glass mix is not ideal, as our results show. The wide range of the Mg/Fe distribution-coefficients for olivine-glass (0.27-0.90) indicates that equilibria for these experiments were not achieved.

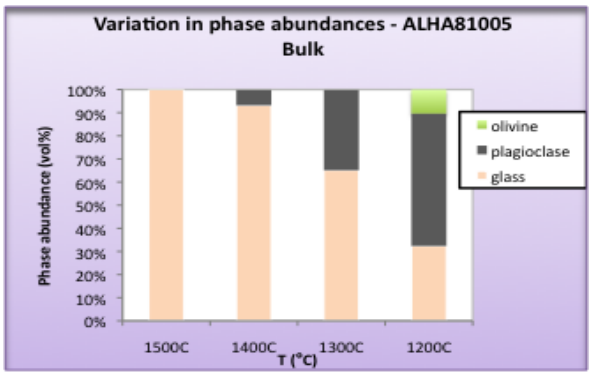

Figure 2: Variation in phase abundances (wt%) for ALHA81005 bulk composition starting mixture at 1 bar as a function of temperature, showing the crystallization of plagioclase and olivine

Table 2: Representative EMP analyses of experiment run products, bulk composition of clast 2.

	1500°C		1400°C			1300°C			1200°C				1150°C				
Wt%	glass	spinel	glass	spinel	olivine	glass	spinel	olivine	glass	spinel	olivine	plag	glass	spinel	olivine	plag	clast2 bulk
SiO_2	39.77	0.66	40.67	0.70	41.76	38.92	0.79	39.28	35.23	0.58	45.77	41.24	45.77	0.27	42.65	45.61	29.50
TiO_2	1.87	0.41	2.51	0.39	0.09	2.16	0.42	0.08	6.62	0.89	0.19	0.15	3.02	0.50	0.18	0.37	0.16
Al_2O_3	16.82	65.86	18.87	64.97	1.09	15.49	60.90	1.50	18.53	67.88	0.54	35.15	13.38	65.77	0.29	34.81	36.00
FeO	10.72	5.63	9.92	7.87	10.48	10.80	6.71	8.22	7.61	10.72	13.99	0.54	2.19	4.94	5.83	0.33	10.10
MnO	0.19	0.11	0.19	0.09	0.17	0.20	0.07	0.12	0.15	0.13	0.26	0.01	0.10	0.09	0.14	0.00	0.15
MgO	19.55	24.84	13.26	23.60	48.70	17.56	25.24	51.07	11.88	21.85	45.77	0.41	14.28	25.12	52.41	0.57	13.85
CaO	11.19	0.15	15.09	0.18	0.53	12.91	12.91	0.52	19.83	0.59	0.98	19.72	21.99	0.14	0.45	19.62	8.60
Na_2O	0.07	0.01	0.04	0.01	0.00	0.02	0.00	0.00	0.03	0.01	0.00	0.14	0.02	0.00	0.00	0.25	0.27
Total	100.17	97.66	100.55	97.80	102.83	98.05	107.04	100.77	99.88	102.65	107.51	97.37	100.75	96.83	101.95	101.57	98.63

Thus we cannot determine whether clast 2 could be a melt composition itself, or if other processes must have taken place in order to enrich this sample in spinel. The maximum spinel crystallization of 30vol% has to be taken in with care. It could be possible that some oxide grains - e.g. Al_2O_3 - served as nucleation grains to crystallize the spinel.

However, the bulk composition plots within the spinel field (though outside this projection), and it is not surprising that spinel is the first phase to crystallize. The next phase to crystallize is olivine at 1400ºC, indicating the melt composition follows the proposed line in Figure 2.

Further experiments using the homogenized glass powder will determine how much vol % spinel can be crystallized. Only then can we determine whether accumulation is a major process in the formation of spinel-rich lithologies.

Acknowledgments: We are grateful to L. Le for her assistance with the 1-bar furnace experiments and to A.H. Treiman for discussion.

References: [1] Taylor (1982) *Planetary Science: A Lunar Perspective*. LPI [2] Demidova et al. (2007) *Petrology* 15, 386-407. [3] Isaacson et al. (2011) *Journal of Geophysical Research* 116, E00G11. [4] Pieters CM., et al. (2010) LPSC 41, #1854. [5] Gross J. and Treiman A.H (2010) 41st LPSC, Abstr. 2180. [6] Rahilly K.E. and Treiman A.H. (2009) LPSC 40, #1168. [7] Goodrich C.A., et al. (1984) *J. Geophys. Res.*, 89, C87-C94. [8] Korotev R.L. (2005) *Chemie der Erde*, 65, 297-346. [9] Korotev R.L. (2004) *Science* 305, 622-623. [10] Gross J. and Treiman A.H. (2011) *Journal of Geophysical Research* 116, E10009. [11] Borisov A. and Jones J.H., (1999) *Am. Mineral.*, 84, 1528-1534. [12] Roeder P.L. and Emslie R.F. (1970) *Contrib. Mineral. Petrol.*, 29, 275-289. [13] Filiberto J. and Dasgupta R. (2010) *Meteor. & Planet. Sci.*, 45, A54.